The Astrophysical Journal, 642:554–561, 2006 May 1


# DETERMINATION OF THE MAGNETIC FIELD VECTOR VIA THE HANLE AND ZEEMAN EFFECTS IN THE He I $\lambda$10830 MULTIPLET: EVIDENCE FOR NEARLY VERTICAL MAGNETIC FIELDS IN A POLAR CROWN PROMINENCE

L. Merenda and J. Trujillo Bueno[1]
Instituto de Astrofísica de Canarias, E-38205 La Laguna, Tenerife, Spain; merenda@iac.es, jtb@iac.es

E. Landi Degl'Innocenti
Dipartimento di Astronomia e Scienza dello Spazio, Università di Firenze, Largo Enrico Fermi 2, I-50125 Firenze, Italy; landie@arcetri.astro.it

and

M. Collados
Instituto de Astrofísica de Canarias, E-38205 La Laguna, Tenerife, Spain; mcv@iac.es
*Received 2005 July 1; accepted 2006 January 5*

## ABSTRACT

The magnetic field is the key physical quantity responsible for the formation, stability, and evolution of solar prominences (ribbons of cool dense gas embedded in the hot tenuous corona). Therefore, it is important to obtain good empirical knowledge of the three-dimensional structure of prominence magnetic fields. Here we show how the magnetic field vector can be inferred via the physical interpretation of spectropolarimetric observations in the He I $\lambda$10830 multiplet. To this end, we have developed an inversion code based on the quantum theory of the Hanle and Zeeman effects and on a few modeling assumptions. We show an application to full Stokes vector observations of a polar crown prominence that, in the slit-jaw H$\alpha$ image, showed nearly vertical plasma structures. Our results provide evidence for magnetic fields on the order of 30 G inclined by about 25° with respect to the local solar vertical direction. Of additional interest is that the inferred nearly vertical magnetic field vector appears to be slightly rotating around a fixed direction in space as one proceeds along the direction of the spectrograph's slit. While these results provide new light on the three-dimensional geometry of the magnetic fields that confine the plasma of polar crown prominences, they also urge us to develop improved solar prominence models and to pursue new diagnostic investigations.

*Subject headings:* stars: magnetic fields — Sun: corona — Sun: prominences

## 1. INTRODUCTION

Solar prominences are relatively cool, dense ribbons of plasma located tens of thousands of kilometers above the visible "surface" of the Sun and embedded in the $10^6$ K solar corona. They represent interesting physical systems in which magnetic fields are interacting with plasma in subtle ways, dense plasma is being supported against gravity, and thermal instabilities and/or continual magnetic flux emergence and reconnection processes might be creating the cool dense gas (e.g., the reviews by Priest 1989; van Ballegooijen 2001). On the other hand, the eruption of a prominence often produces a coronal mass ejection, which may have a dramatic influence on near-Earth space weather. Therefore, it is very important to obtain good empirical knowledge of the three-dimensional structure of prominence magnetic fields.

The most reliable strategy we have available for inferring the magnetic field vector is via the measurement and theoretical interpretation of Stokes profiles in suitably chosen spectral lines. The quantum theory of the Hanle and Zeeman effects for the interpretation of spectropolarimetric observations started to be developed many years ago (e.g., Bommier 1976, 1980; Landi Degl'Innocenti 1982), and it is of interest to mention that it has been described in great detail in a very recent monograph (Landi Degl'Innocenti & Landolfi 2004). Most of the modern work concerning the diagnostics of prominence magnetic fields has been carried out via the He I D3 multiplet at 5876 Å whose polarization is mainly governed by scattering processes and the Hanle effect (e.g., the reviews by Leroy 1989; Landi Degl'Innocenti 1990; Paletou & Aulanier 2003 and references therein). For instance, inversion of new spectropolarimetric observations in the He I D3 multiplet has been applied to obtain two-dimensional maps of the magnetic field vector (López Ariste & Casini 2002; Casini et al. 2003). Our work in this research field is based, however, on spectropolarimetry of the He I $\lambda$10830 multiplet, which offers an attractive diagnostic window for deciphering the three-dimensional geometry of the magnetic field confining the prominence plasma (Lin et al. 1998; Trujillo Bueno et al. 2002) and of that channeling the spicular motions (Trujillo Bueno et al. 2005).

The Tenerife Infrared Polarimeter allows us to measure the four Stokes parameters with a high degree of sensitivity in near-IR spectral lines. Using this instrument attached to the German Vacuum Tower Telescope and modeling the observed spectral line polarization within the framework of the quantum theory of the Hanle and Zeeman effects, we are investigating the three-dimensional structure of the magnetic fields that confine the plasma of solar coronal filaments and prominences.

The aim of this paper is twofold: first, to summarize our approach to the difficult problem of the determination of the magnetic field vector from the observed polarization in the He I $\lambda$10830 multiplet; second, to report that the magnetic field vector in a polar crown prominence consisting of several vertical threads of plasma was found to be rotating around a fixed direction in space, when considering consecutive spatial points along the direction specified by the spectrograph's slit. As we show below, the mean inclination (with respect to the vertical) of the inferred magnetic field vector turns out to be about 25° when the observed prominence plasma is assumed to be in the plane of the sky,

[1] Consejo Superior de Investigaciones Científicas (Spain).

which, as discussed below, is an assumption suggested by synoptic H$\alpha$ maps of the observed polar crown prominence. This finding is of great scientific interest because of the widespread belief that the magnetic field vector that allows the very existence of solar prominences is always practically horizontal. In our opinion, this statement might not hold for polar crown prominences with curtain-like vertical plasma structures like the one we have observed.

Before entering into details, it is convenient to recall briefly the magnetic field diagnostics work of previous authors on polar crown prominences. First of all, it is important to point out that the determination of the magnetic field in 120 prominences of the polar crown carried out by Leroy et al. (1983) was based on the interpretation of broadband linear polarization data in the He I $D_3$ line, which makes it impossible to determine completely the magnetic field vector because only the integrated values of $Q/I$ and $U/I$ in a single line were used. For this reason, the authors were forced to assume that the magnetic field vector was horizontal and determined both the strength and the azimuth within the framework of this horizontal-field hypothesis. Later, Bommier et al. (1994) interpreted the broadband linear polarization of 10 polar crown prominences observed quasi-simultaneously in the He I D3 and H$\alpha$ lines. In principle, with this type of polarimetric data it should be possible to determine the three components of the magnetic field vector (strength, inclination, and azimuth), since the two lines have different sensitivities to the Hanle effect (Bommier et al. 1981). However, one of the serious problems is that the H$\alpha$ line is optically thick, which implies that the determination of the magnetic field vector is strongly model dependent. In particular, the determination of Bommier et al. (1994) was based on radiative transfer calculations in a given solar prominence model (Landi Degl'Innocenti et al. 1987). An indication of the complexity of the diagnostic problem under consideration is that for the optically thick H$\alpha$ line the zero-field polarization direction is not the parallel to the solar limb. On the basis of such modeling assumptions Bommier et al. (1994) carried out a very detailed analysis of the above-mentioned observations and concluded that the average field strength in the observed polar crown prominences was about 7 G and that the average inclination angle with respect to the local solar vertical was 60°. Finally, it is also of interest to mention that Athay et al. (1983), Querfeld et al. (1985), and Casini et al. (2003) concluded that the inferred magnetic field vectors from Stokes profile observations of the He I D3 multiplet were found to be mostly horizontal, but to the best of our knowledge none of the observed prominences were of the polar crown type. Practically horizontal fields were also found by Trujillo Bueno et al. (2002) in a solar coronal filament that was located at the very center of the solar disk during the day of observation. This result was obtained via the physical interpretation of spectropolarimetric observations of the Hanle and Zeeman effects in the He I $\lambda$10830 multiplet.

The outline of this paper is as follows. After a brief description of the observations (§ 2) we discuss in some detail in § 3 our approach to the theoretical modeling of the Hanle and Zeeman effects in optically thin solar prominences, showing some examples of model calculations that illustrate the behavior of the linear and circular polarization signatures. Finally, after highlighting our Stokes-inversion strategy in § 4, we present our main results and conclusions in § 5.

## 2. SPECTROPOLARIMETRIC OBSERVATIONS OF A POLAR CROWN PROMINENCE

The observations reported here were carried out on 2001 May 27 with the Tenerife Infrared Polarimeter (TIP; see Martínez Pillet et al. 1999) mounted on the German Vacuum Tower Telescope of the Observatorio del Teide (Tenerife, Spain). TIP uses ferroelectric liquid crystal retarders as polarization modulators. After the light beam is temporally modulated it goes through a double birefringent plate that divides it into two orthogonal polarization beams, which are then imaged on a single detector array. In order to measure $I$, $Q$, $U$, and $V$, TIP takes four consecutive images with independent analyzer configurations, which results in linear combinations of the four Stokes parameters. The information obtained independently from each polarization beam is combined only at the end of the data reduction procedure in order to correct for the seeing-induced cross talk from $I$ to $Q$, $U$, and $V$.

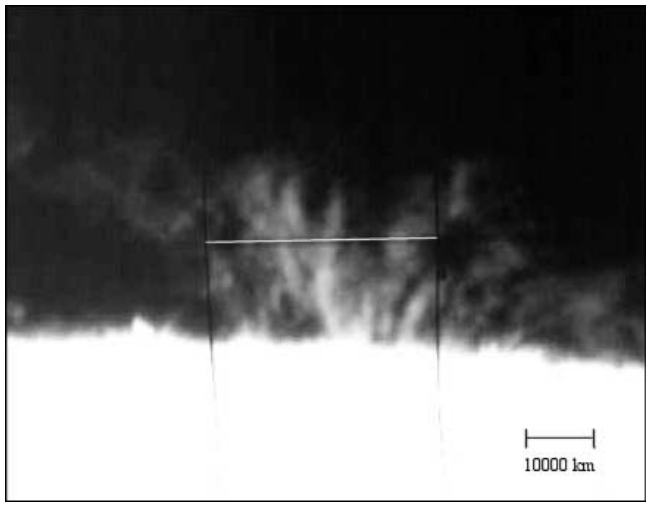


FIG. 1.—Slit-jaw image of the observed prominence. The white line indicates the location of the spectrograph's slit.

The spectrograph slit was located about 20″ off the south solar visible limb and parallel to it, thus crossing the prominence material as indicated in Figure 1. This H$\alpha$ slit-jaw image shows that the observed polar crown prominence consisted of several nearly vertical threads of plasma. The observed prominence points, which correspond to the central part of the various prominence features seen in Figure 1, were located rather close to the plane of the sky, as suggested by synoptic H$\alpha$ maps from Big Bear Solar Observatory.

For that fixed slit position we took a time series of 40 consecutive images, each image resulting from the accumulation of 10 snapshots of 250 ms. We also took a series of polarimetric calibration images in order to correct for the instrumental polarization of the telescope (see Collados 2003). Any residual $I$ to $Q$, $U$, and $V$ cross talk was removed by setting to zero the continuum polarization. In order to improve the signal-to-noise ratio we temporally averaged the 40 consecutive images of the time series observed. Figure 2 shows the observed Stokes parameters of the He I $\lambda$10830 multiplet at one point along the direction of the spectrograph's slit. This multiplet results from transitions between the metastable term $2^3S$ (which has a single level with total angular momentum $J = 1$) and the term $2^3P$ (which has three levels with $J = 2$, 1, 0 in order of increasing energy). Therefore, it has three spectral lines: a "blue" line at 10829.09 Å (with $J_l = 1$ and $J_u = 0$) and two "red" lines, at 10830.25 Å (with $J_u = 1$) and at 10830.34 Å (with $J_u = 2$), which appear blended at the plasma temperatures of solar prominences. Note that only the red line shows a significant linear polarization signal.

We find that Stokes $Q$ and Stokes $U$ do not show large variations in the observed prominence. In particular, $Q$ is always

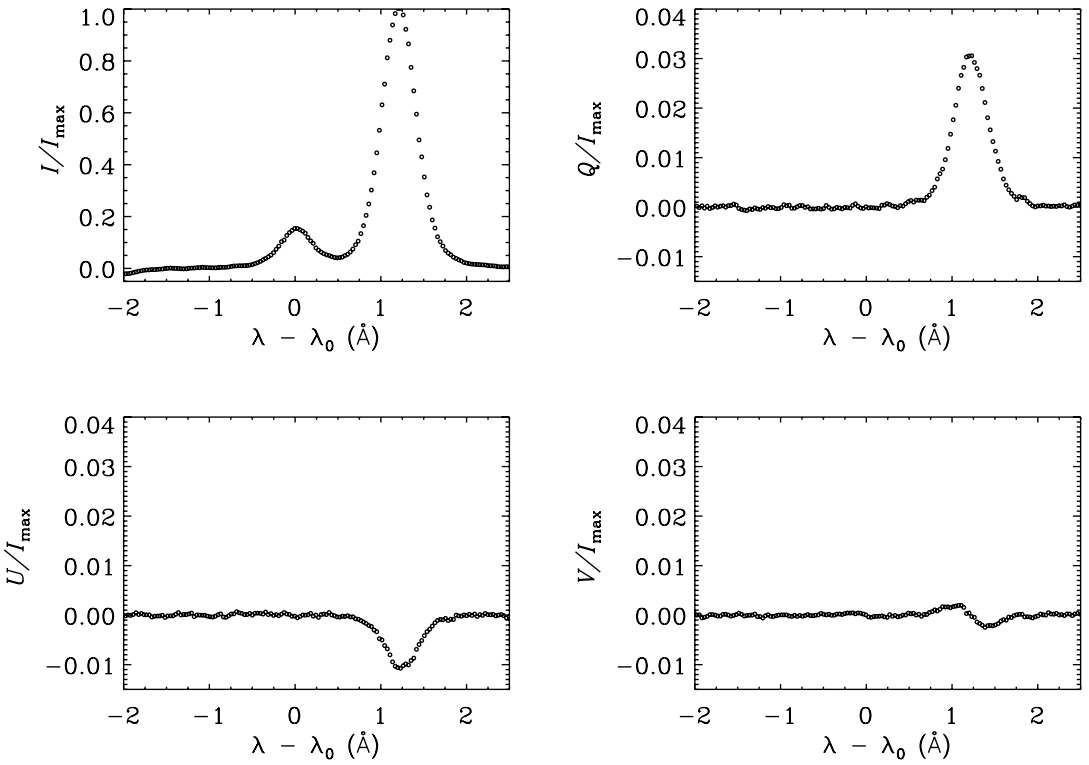


FIG. 2.—Example of the observed Stokes profiles of the He I $\lambda$10830 multiplet corresponding to a point along the slit. The positive reference direction for Stokes $Q$ is the parallel to the solar limb. The zero of the wavelength axis is set to the center of the blue line (see text).

positive and $U$ is always negative. Finally, note that the amplitudes of the Stokes $V$ signals were significant.

## 3. THEORETICAL MODELING OF THE HANLE AND ZEEMAN EFFECTS IN SOLAR PROMINENCES

To infer the magnetic field vector in solar prominences from the observed Stokes profiles in the He I $\lambda$10830 multiplet, we apply the theory of the Hanle and Zeeman effects as described in detail in Landi Degl'Innocenti & Landolfi (2004). The multiterm model atom that we adopt is the same as that shown in Figure 13.9 of the book just quoted. The main assumptions of our analysis are that the prominence plasma is optically thin and that collisions play a negligible role in the atomic excitation. The key process taken into account is the interaction between the He I atoms in the prominence plasma and the anisotropic radiation field coming from the underlying solar photosphere. The ensuing pumping by anisotropic radiation induces population imbalances and quantum coherences among the magnetic substates of the energy levels (that is, atomic polarization), which we quantify by solving the statistical equilibrium equations for the multipole components $\rho^K_Q(J,\ J')$ of the atomic density matrix (see § 7.6.a in Landi Degl'Innocenti & Landolfi 2004). Such equations take fully into account the effects produced by a static magnetic field of given strength $B$, inclination $\theta_B$, and azimuth $\chi_B$ (see Fig. 3). We point out that the atomic level polarization (and the ensuing emergent spectral line polarization) is modified by the Hanle effect (e.g., the review by Trujillo Bueno 2001).

We have solved the statistical equilibrium equations by assuming that the helium atoms (located at the observed prominence height above the visible solar limb) are radiatively excited by the given continuum radiation coming from the underlying solar photosphere, whose center-to-limb variation has been tabulated by Pierce (2000). Moreover, we have assumed that the observed points in the prominence are located in the plane of the sky (i.e., in Fig. 3 the aspect angle $\delta = 0^\circ$).[2]

From the calculated density matrix elements it is then possible to compute the emission coefficients $\epsilon_i$ (with $i = I, Q, U, V$) for the line transition under consideration (see the equations of § 7.6.b in Landi Degl'Innocenti & Landolfi 2004). It is then straightforward to calculate the emergent Stokes parameters because, for an optically thin medium, they are simply proportional to the

[2] As mentioned in § 2, we have some clear hints that indicate that the observed prominence points were located rather close to the plane of the sky. In any case, we explain in § 4 the reasons why we believe that our conclusion of slightly inclined magnetic fields in the polar crown prominence plasma we observed on 2001 May 27 remains valid even if $\delta$ were as large as 15°.

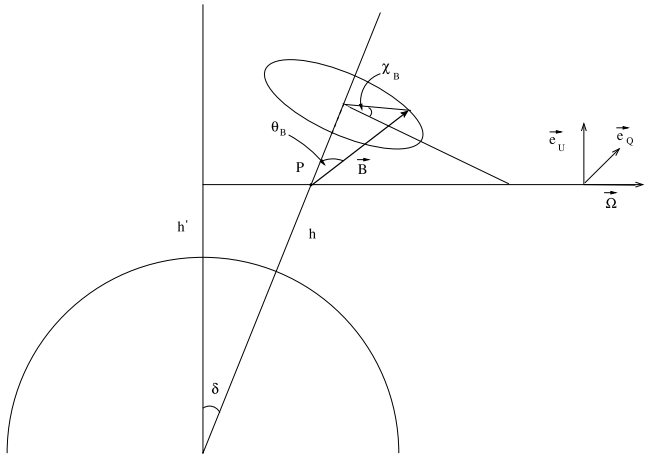


FIG. 3.—Geometry of the problem, indicating the inclination ($\theta_B$) and azimuth ($\chi_B$) of the magnetic field vector at the observed spatial point.

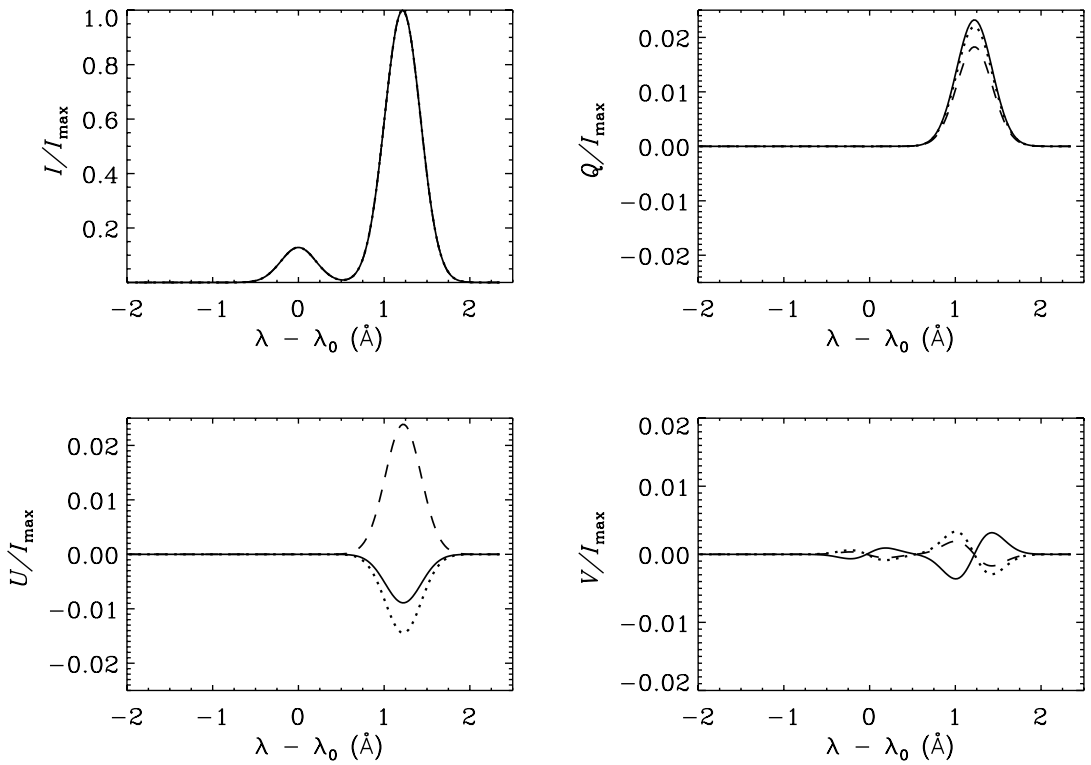


FIG. 4.—Stokes profiles of the He I $\lambda$10830 multiplet resulting from our theoretical scheme. The profiles were computed for $h = 20''$, $B = 40$ G, and $\theta_B = 30^\circ$. The solid, dashed, and dotted lines refer respectively to $\chi_B = 20^\circ$, $240^\circ$, and $150^\circ$. In all cases we used a thermal velocity $v_T = 8$ km s$^{-1}$.

corresponding components of the emission vector. It is also important to point out that we have calculated the wavelength positions and strengths of the Zeeman components in the incomplete Paschen-Back effect regime, as described in detail in Landi Degl'Innocenti & Landolfi (2004). Therefore, our approach is valid for a broad range of magnetic field strengths, which allows us to investigate rigorously the joint action of both the Hanle and Zeeman effects in all the lines of the assumed multiterm model atom.

Figure 4 shows a theoretical example of the Stokes profiles obtained through the method outline above. It is noteworthy that Stokes $Q$ is positive for the three magnetic field configurations considered in the figure, while the sign of Stokes $U$ is very sensitive to the value of the magnetic field azimuth. It is also of interest to point out that the calculated ratio $I_{red}/I_{blue}$ is $\approx$8 under our assumption of an optically thin medium, which is only slightly larger than the observed one (see Fig. 2). We also point out that a similar ratio was found for all the observed intensity profiles.

### 3.1. *Linear Polarization*

In an optically thin medium the linear polarization produced by scattering processes results from selective emission processes, which are due to the presence of atomic polarization in the upper level of the spectral line under consideration (see Trujillo Bueno et al. 2002). For this reason, in Figures 2 and 4 the blue line of the He I $\lambda$10830 multiplet does not show any linear polarization, given that its upper level has $J_u = 0$ and is therefore intrinsically unpolarizable.

In order to describe the magnetic field dependence of the linear polarization in the red line, it is convenient to distinguish between two magnetic field intensity regimes: the "Hanle effect sensitive" regime and the "saturated Hanle effect" regime. In the Hanle-effect-sensitive regime, the linear polarization signal is affected by both the intensity and the direction of the magnetic field, while in the saturated regime it is only sensitive to its direction. For the red line of the He I $\lambda$10830 multiplet the transition between these two regimes occurs for a magnetic strength of about 8 G.

Figure 5 shows the magnetic field dependence of the linear polarization amplitude for the Hanle-effect-sensitive regime. In this Hanle effect diagram solid lines indicate the ratios $Q/I$ and $U/I$ at the line core of the red blended component, calculated for constant values of $\chi_B$ with the magnetic field intensity ($B$) ranging from 0 to 10 G, while dotted lines correspond to constant values of $B$ with the azimuth $\chi_B$ ranging from $0^\circ$ to $180^\circ$. All curves of the diagram are calculated for the case of a horizontal

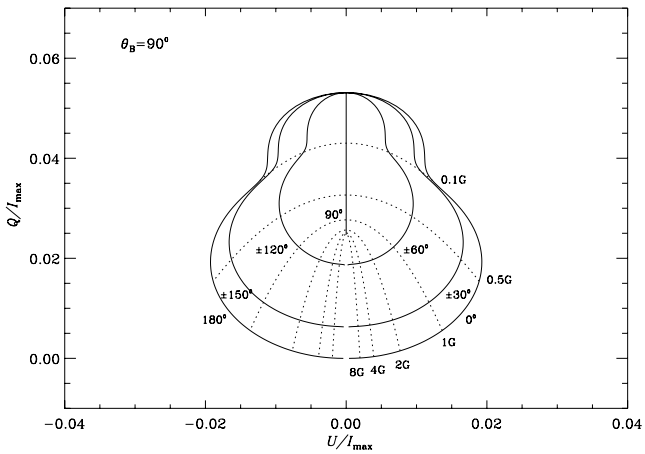


FIG. 5.—Theoretical Hanle effect diagram for the line core of the red blended component of the He I $\lambda$10830 multiplet. The calculations have been carried out for $h = 20''$ and $\theta_B = 90^\circ$, and assuming a thermal velocity $v_T = 8$ km s$^{-1}$. Solid lines correspond to constant values of the azimuth $\chi_B$, with the magnetic strength ranging from 0 to 10 G. Dotted lines refer to constant values of the magnetic field intensity with $\chi_B$ ranging from $0^\circ$ to $180^\circ$.

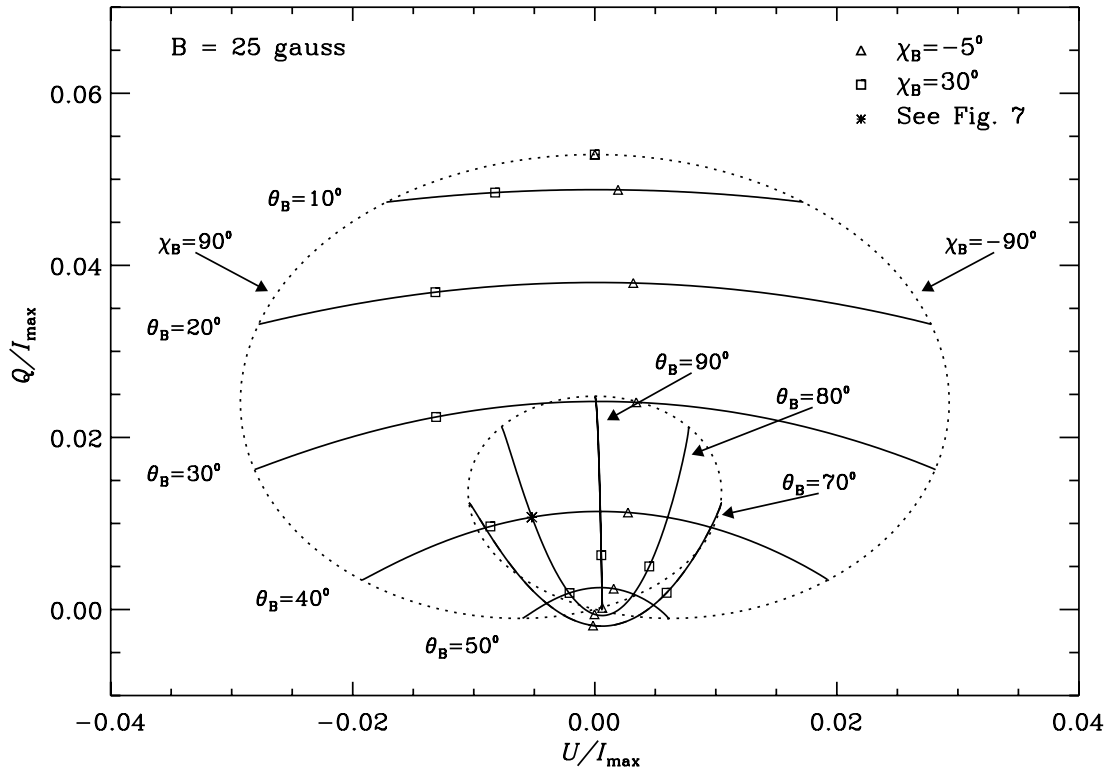


FIG. 6.—Theoretical Hanle effect diagram for the saturation regime of the red blended component of the He I $\lambda$10830 multiplet. The calculations have been performed for $B = 25$ G. Solid lines correspond to constant values of $\theta_B$, with magnetic field azimuth $\chi_B$ varying between $-90^\circ$ and $90^\circ$. The triangles indicate points corresponding to $\chi_B = -5^\circ$ on these solid lines, while the squares indicate points corresponding to $\chi_B = 30^\circ$. Dotted lines refer to constant values of $\chi_B$ ($\chi_B = \pm 90^\circ$), with the inclination $\theta_B$ varying between $0^\circ$ and $90^\circ$. Finally, the asterisk indicates the common position on this diagram of the combination of angles producing the profiles shown in Fig. 7. An identical diagram would result from the transformation $\theta_B \rightarrow 180^\circ - \theta_B$, $\chi_B \rightarrow -\chi_B$. Note that the same diagram would also result from the further transformation $\chi_B \rightarrow 180^\circ - \chi_B$. However, this transformation leaves invariant the linear polarization Stokes parameters $Q$ and $U$ but changes the sign of the circular polarization so that it does not introduce a further ambiguity.

magnetic field ($\theta_B = 90^\circ$). The prominence plasma is supposed to be located in the plane of sky at a height of $20''$ above the visible solar limb, which is the height of the spectrograph's slit seen in the slit-jaw H$\alpha$ image of the observed prominence (see Fig. 1).

Figure 6 shows instead the magnetic field dependence of the linear polarization amplitude in the saturated regime. Here we consider the case of a constant magnetic field ($B = 25$ G). Solid lines correspond to constant values of the inclination $\theta_B$ with the azimuth $\chi_B$ ranging from $-90^\circ$ to $90^\circ$, while dotted lines indicate constant values of $\chi_B$ with the inclination $\theta_B$ ranging from $0^\circ$ to $90^\circ$.

In this Hanle effect diagram it is very important to note the existence of an ambiguity region in which one can have pairs of similar emergent Stokes profiles corresponding to different magnetic field vectors. This so-called Van Vleck ambiguity was pointed out by House (1977) and Casini & Judge (1999) concerning the scattering polarization in forbidden coronal lines, and it adds to the familiar ambiguity mentioned in the figure legends. As seen in Figure 6, when we are in the saturation regime we can have similar $Q/I$ and $U/I$ profiles for two different values of the magnetic field vectors with inclination $\theta_B$ such that $\theta_1 < \theta_B < \theta_2$ (with $\theta_1 \approx 30^\circ$ and $\theta_2 \approx 150^\circ$). We point out that for inclinations $30^\circ \lesssim \theta_B < 54.^\circ7$ (or $125.^\circ3 < \theta_B \lesssim 150^\circ$) the existence of the Van Vleck ambiguity is restricted to a narrow interval of $\chi_B$ values. For instance, for $\theta_B = 40^\circ$ there is no ambiguity if $30^\circ \lesssim \chi_B \leq 90^\circ$ or if $-90^\circ \leq \chi_B \lesssim -30^\circ$. Figure 7 shows an example of similar Stokes profiles that are produced by two different magnetic field vectors. Unfortunately, this Van Vleck ambiguity cannot be solved by using the observed circular polarization profile because, as is explained in the next section, the longitudinal component of the magnetic field can be adjusted to fit the observed Stokes $V$ profile by simply increasing or decreasing its strength. Note that this does not affect the linear polarization because we are in the saturation regime.

### 3.2. *Circular Polarization*

Two mechanisms are capable of inducing circular polarization in the spectral lines observed in prominences: the longitudinal Zeeman effect and the presence of atomic orientation, that is, the existence of an unequal population of the Zeeman sublevels with $M > 0$ with respect to those with $M < 0$, which is in turn produced by the so-called alignment-to-orientation mechanism. When the intensity of the magnetic field is sufficiently weak (splitting of magnetic sublevels is small with respect to the width of the spectral line) and atomic orientation is negligible, the Stokes $V(\lambda)$ profile tends to be antisymmetric, since it is approximately given in each component by (e.g., Landi Degl'Innocenti & Landolfi 2004)

$$V(\lambda) \approx -\Delta\lambda_B \bar{g} \cos\psi \frac{dI(\lambda)}{d\lambda}, \quad (1)$$

where $\Delta\lambda_B = 4.67 \times 10^{-13} \lambda^2 B$ (with $\Delta\lambda_B$ and $\lambda$ in angstroms and $B$ in gauss), $\bar{g}$ is the effective Landé factor of the single-line component under consideration, and $\psi$ the angle between the magnetic field vector and the line of sight ($\cos\psi = \sin\theta_B \cos\chi_B$).

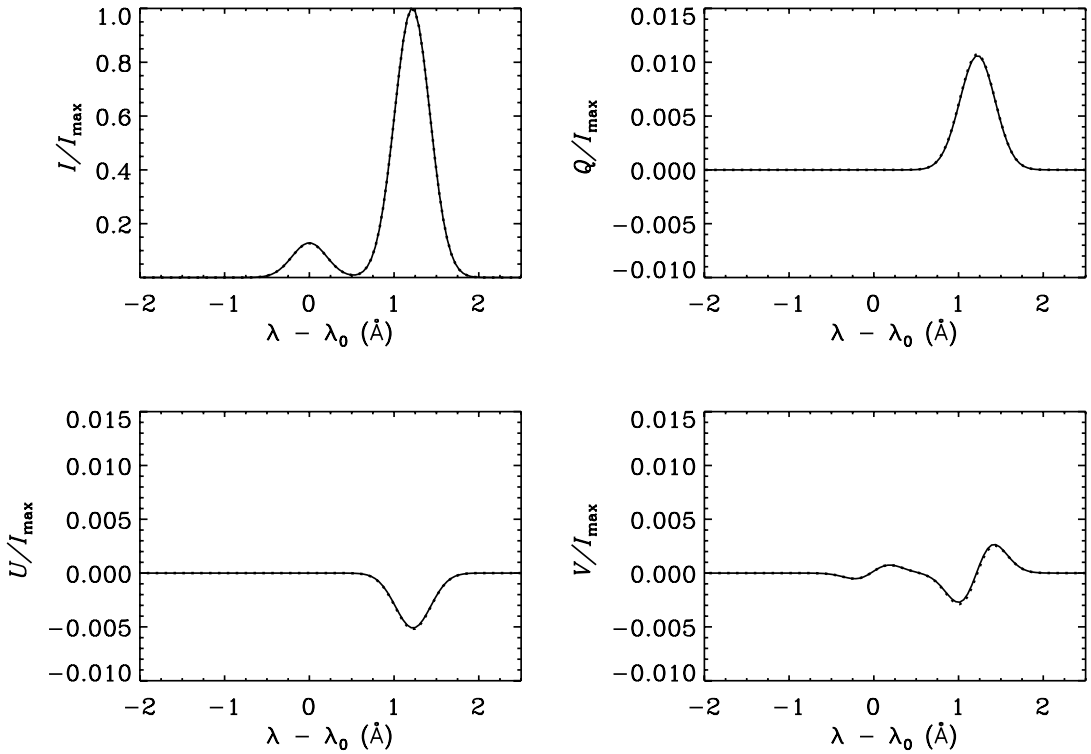


FIG. 7.—Example of the Van Vleck ambiguity showing two similar Stokes profiles that correspond to two different magnetic field vectors. The solid line refers to a magnetic field vector with $\theta_B = 80^\circ$, $\chi_B = -46^\circ$, and $B = 22$ G, while the dotted line corresponds to $\theta_B = 40^\circ$, $\chi_B = 19^\circ$, and $B = 25$ G. The asterisk in Fig. 6 indicates the position corresponding to these two magnetic field vectors in the Hanle effect saturation diagram. As in all previous figures, we have assumed a thermal velocity $v_T = 8$ km s$^{-1}$ and $h = 20''$. Note also that the Van Vleck ambiguity adds to the "traditional" one, so that there are indeed four magnetic field vectors that produce the same polarization profile. Besides the two just quoted, the other possibilities are ($B = 22$ G, $\theta_B = 100^\circ$, $\chi_B = 46^\circ$) and ($B = 25$ G, $\theta_B = 140^\circ$, $\chi_B = -19^\circ$).

On the contrary, the presence of a sizable amount of atomic orientation tends to produce a $V(\lambda)$ profile of the form

$$V(\lambda) = \alpha\,\phi(\lambda),$$

where $\phi(\lambda)$ is a symmetric profile and $\alpha$ is a coefficient that depends of the amount of atomic orientation present in the energy levels of the transition under consideration. For the $\lambda$10830 multiplet observed in prominences, where the magnetic field intensity is typically smaller than 100 G, the effect of atomic orientation is insignificant. This can be seen in Figure 8, which shows only a small difference between the rigorously calculated $V(\lambda)$ profile (*dotted line*) and that obtained via equation (1) (*solid line*), which is nothing but the weak-field approximation of the Zeeman effect.

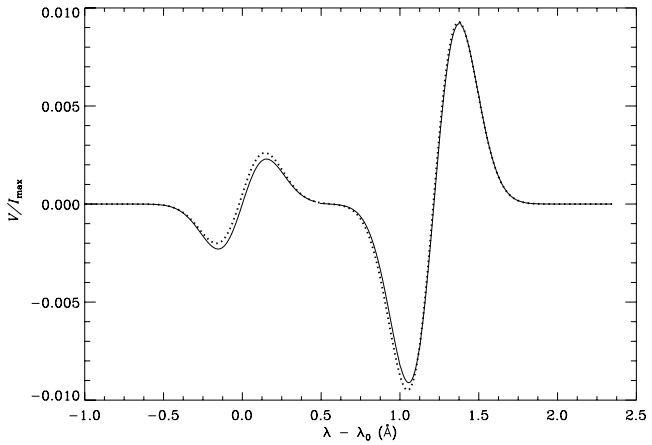


FIG. 8.—Comparison between the theoretical $V$ profile computed according to eq. (1) (*solid line*) and that obtained by means of the rigorous theory detailed in the text (*dotted line*). The rigorous calculation corresponds to a 40 G longitudinal field ($\theta_B = 90^\circ$, $\chi_B = 0^\circ$). The approximated Stokes $V$ profile was obtained by using $\bar{g} = 2$ for the blue line and $\bar{g} = 1.1$ for the red line. As in all previous figures, $h = 20''$ and $v_T = 8$ km s$^{-1}$.

## 4. DETERMINATION OF THE MAGNETIC FIELD VECTOR VIA A STOKES-INVERSION STRATEGY

In order to infer the magnetic field vector we compare the observed Stokes profiles at each point along the slit with the theoretical Stokes parameters included in a suitable database, which we have carefully created to facilitate a fast and precise determination. To this end, we have taken advantage of the fact that for each observed point, we found that we are in the saturation regime of the upper-level Hanle effect, since we systematically found $B_{||} \geq 8$ G via the application of equation (1).

This allowed us to create a simpler database by using a single magnetic field strength (i.e., 25 G) and calculating the emergent Stokes $Q$ and $U$ profiles for all the orientations of the magnetic field vector in space. The magnetic field direction could be found by confronting the observed linear polarization profiles with the theoretical ones. Once the magnetic field direction was found, we obtained its intensity by fitting the Stokes $V$ profile.[3] Figure 9 shows an example of the good fit we were able to obtain via the application of this Stokes-inversion technique.

Figure 10 shows all the $Q/I$ and $U/I$ line-center values of the linear polarization profiles contained in our theoretical database. In addition, in this figure we also indicate the points corresponding to the observed values. As seen in the figure, all the observed

[3] We point out that increasing or decreasing the strength of the magnetic field does not change the linear polarization when we are in the saturation regime of the Hanle effect.

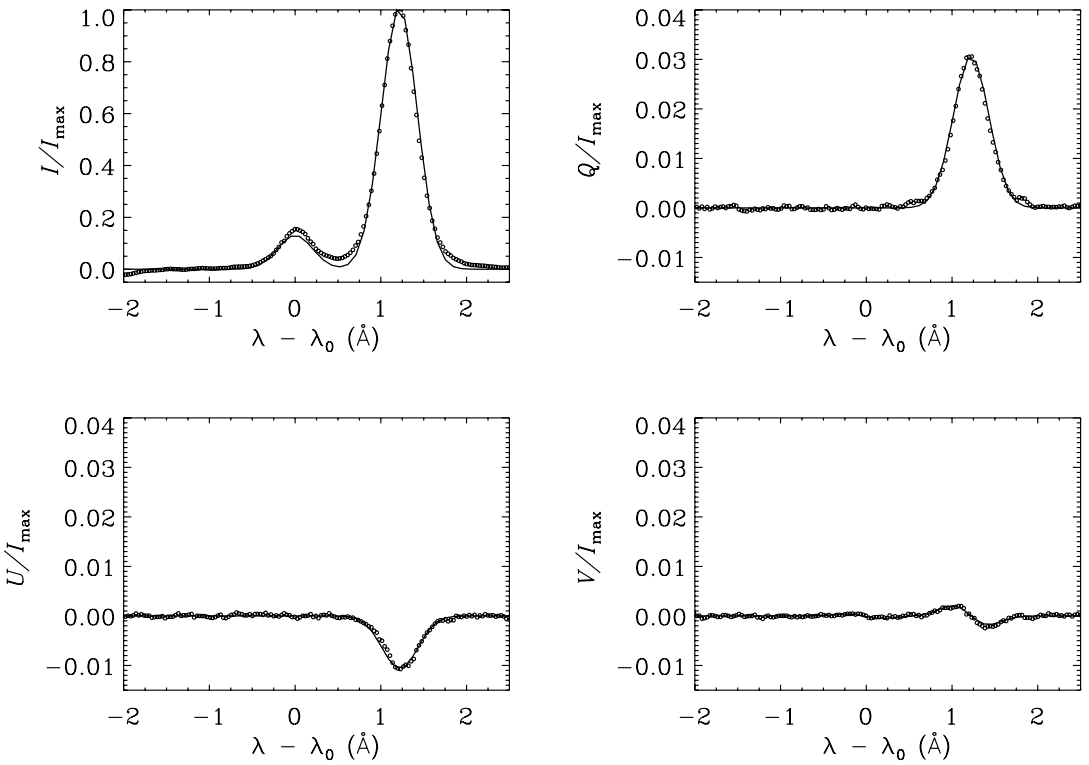


FIG. 9.—Example of the goodness of the theoretical fit (*solid line*) to the observed Stokes profiles of Fig. 2 (*open circles*). The theoretical Stokes profile corresponds to $B = 31$ G, $\theta_B = 25^\circ$, and $\chi_B = 160\overset{\circ}{.}5$, or to the "classical ambiguity" set ($B = 31$ G, $\theta_B = 155^\circ$, $\chi_B = -160\overset{\circ}{.}5$).

values lie outside the Van Vleck ambiguity region previously discussed in § 3.1. However, it is important to point out that this applies to the case of our basic assumption, that is, that the prominence plasma is located in the plane of the sky ($\delta = 0^\circ$). In fact, the larger the aspect angle $\delta$ of Figure 3, the larger the height $h$ and the larger both the degree of anisotropy of the pumping radiation field and the linear polarization amplitude of the scattered radiation. This raises the question of whether or not the observed $Q/I_{max}$ and $U/I_{max}$ values are actually lying inside the Van Vleck ambiguity region corresponding to the real $\delta$-value of the observed prominence, in which case we would not be able to distinguish between nearly vertical and nearly horizontal magnetic fields. In order to determine how large the aspect angle $\delta$ should be in order that our observation fall in the ambiguity region, we have carried out a detailed investigation using databases corresponding to increasing $\delta$-values. As a result, we have found that $\delta$ would have to be larger than 15° (corresponding to $h = 54\overset{''}{.}5$) in order to have all the observed points inside the corresponding Van Vleck ambiguity region. Such a large $\delta$-value seems very unlikely to us, given that synoptic H$\alpha$ maps from Big Bear Solar Observatory show that the polar crown prominence we observed was moving parallel to the southern limb during the observing period.

The main result of our investigation (based on the assumption $\delta = 0^\circ$) is contained in Figure 11, which shows that the inferred nearly vertical magnetic field vector in the central part of the slit has a strength between 20 and 40 G and is rotating around a fixed direction in space (given by $\bar{\theta}_B \approx 25^\circ$ and $\bar{\chi}_B \approx 168^\circ$) as one considers consecutive spatial points along the direction specified

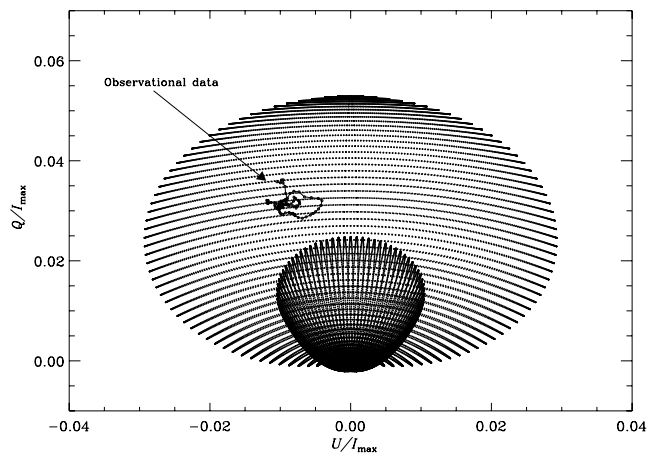


FIG. 10.—Showing that the Stokes profiles of the observed prominence points lie outside the Van Vleck ambiguity region.

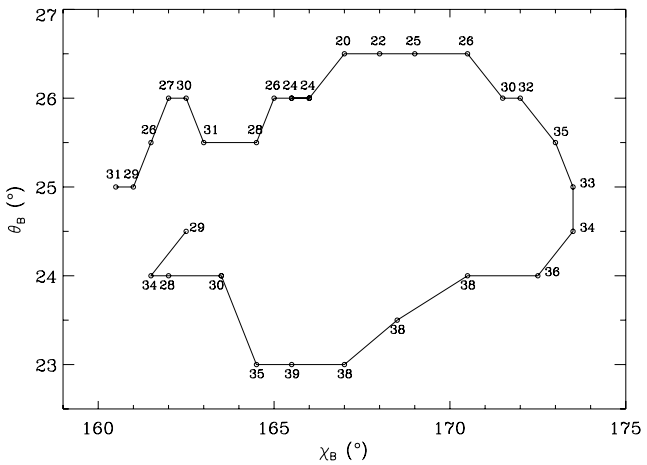


FIG. 11.—Variation along the central part of the spectrograph slit of the inclination ($\theta_B$), azimuth ($\chi_B$), and intensity (in gauss; see the numbers close to each point) of the inferred magnetic field vector when the prominence is assumed to be located in the plane of the sky (i.e., aspect angle $\delta = 0^\circ$).

by the spectrograph's slit. In order to give some information on the sensitivity of the inferred magnetic field vector to the assumed $\delta$-value, we point out that if $\delta$ were $10^\circ$, then the average inclination $\theta_B$ would be about $32^\circ$ and the magnetic strength would be smaller (i.e., between 15 and 30 G, approximately).

## 5. CONCLUSIONS

We have reported spectropolarimetric observations of a polar crown prominence in the He I $\lambda$10830 multiplet, including our physical interpretation of the observed Stokes profiles via the application of an inversion strategy based on the quantum theory of the Hanle and Zeeman effects and on a few (reasonable) modeling assumptions. The observed polar crown prominence showed nearly vertical plasma threads in the slit-jaw H$\alpha$ image (see Fig. 1). As reviewed in § 1, most solar physicists believe that the magnetic field in this type of polar crown prominence is weak (i.e., with $B \approx 10$ G) and substantially inclined with respect to the local solar vertical (i.e., with $\theta_B \geq 60^\circ$). Our results for the polar crown prominence that we observed on 2001 May 27 are significantly different. We infer slightly inclined magnetic fields (with a mean inclination $\bar{\theta}_B \approx 24^\circ.5$ and a mean azimuth $\bar{\chi}_B \approx 168^\circ$). Moreover, as shown in Figure 11, we find that in the central part of the observed polar crown prominence the magnetic field vector is rotating around a fixed direction in space given by $\bar{\theta}_B \approx 25^\circ$ and $\bar{\chi}_B \approx 168^\circ$. It is important to emphasize that, as clarified in the previous section, we do not think that our result (i.e., slightly inclined fields) is an artifact of our assumption that the observed prominence was located in the plane of the sky. In any case, it is important to emphasize that if the aspect angle $\delta$ were larger than $15^\circ$, it would be impossible to distinguish between nearly vertical and nearly horizontal magnetic fields. We have given the arguments that lead us to believe that for the polar crown prominence we observed, $\delta$ was smaller than $15^\circ$.

Our results suggest that the widespread belief that prominence magnetic fields are mainly horizontal might perhaps be valid only for quiescent prominences located far away from the solar magnetic poles. Only a similar theoretical analysis of systematic observations of polar crown prominences, performed at different phases of the solar cycle with high-sensitivity spectropolarimeters, could definitely clarify whether or not the prominence we observed was indeed a rare exception.

This work was partly supported by the Spanish Ministerio de Ciencia y Tecnología through project AYA2004-05792 and by the European Commission via the Solar Magnetism Network. We thank Matt Penn for suggesting useful improvements to an earlier version of this paper.

## REFERENCES

Athay, R. G., Querfeld, C. W., Smartt, R. N., Landi Degl'Innocenti, E., & Bommier, V. 1983, Sol. Phys., 89, 3
Bommier, V. 1976, Ph.D. thesis, Univ. Paris VI
———. 1980, A&A, 87, 109
Bommier, V., Landi Degl'Innocenti, E., Leroy, J. L., & Sahal-Bréchot, S. 1994, Sol. Phys., 154, 231
Bommier, V., Sahal-Bréchot, S., & Leroy, J. L. 1981, A&A, 100, 231
Casini, R., & Judge, P. G. 1999, ApJ, 522, 524
Casini, R., López Ariste, A., Tomczyk, S., & Lites, B. W. 2003, ApJ, 598, L67
Collados, M. 2003, Proc. SPIE, 4843, 55
House, L. L. 1977, ApJ, 214, 632
Landi Degl'Innocenti, E. 1982, Sol. Phys., 79, 291
———. 1990, in IAU Colloq. 117, Dynamics of Quiescent Prominences, ed. V. Ruzdjak & E. Tandberg-Hanssen (Berlin: Springer), 206
Landi Degl'Innocenti, E., Bommier, V., & Sahal-Bréchot, S. 1987, A&A, 186, 335
Landi Degl'Innocenti, E., & Landolfi, M. 2004, Polarization in Spectral Lines (Dordrecht: Kluwer)
Leroy, J. L. 1989, in Dynamics and Structure of Quiescent Solar Prominences, ed. E. Priest (Dordrecht: Kluwer), 77
Leroy, J. L., Bommier, V., & Sahal-Bréchot, S. 1983, Sol. Phys., 83, 135
Lin, H., Penn, M., & Kuhn, J. R. 1998, ApJ, 493, 978
López Ariste, A., & Casini, R. 2002, ApJ, 575, 529
Martínez Pillet, V., et al. 1999, in ASP Conf. Ser. 183, High Resolution Solar Physics: Theory, Observations, and Techniques, ed. T. R. Rimmele, K. S. Balasubramaniam, & R. R. Radick (San Francisco: ASP), 264
Paletou, F., & Aulanier, G. 2003, in ASP Conf. Ser. 307, Third International Workshop on Solar Polarization, ed. J. Trujillo Bueno & J. Sánchez Almeida (San Francisco: ASP), 458
Pierce, K. 2000, in Allen's Astrophysical Quantities, ed. A. N. Cox (4th ed.; New York: AIP), 355
Priest, E. 1989, in Dynamics and Structure of Quiescent Solar Prominences, ed. E. Priest (Dordrecht: Kluwer), 1
Querfeld, C. W., Smartt, R. N., Bommier, V., Landi Degl'Innocenti, E., & House, L. L. 1985, Sol. Phys., 96, 277
Trujillo Bueno, J. 2001, in ASP Conf. Ser. 236, Advanced Solar Polarimetry: Theory, Observation, and Instrumentation, ed. M. Sigwarth (San Francisco: ASP), 161
Trujillo Bueno, J., Landi Degl'Innocenti, E., Collados, M., Merenda, L., & Manso Sainz, R. 2002, Nature, 415, 403
Trujillo Bueno, J., Merenda, L., Centeno, R., Collados, M., & Landi Degl'Innocenti, E. 2005, ApJ, 619, L191
van Ballegooijen, A. A. 2001, in Encyclopedia of Astronomy and Astrophysics, ed. P. Murdin (London: Nature Publishing Group), 2703